J. Coat. Technol. Res., **20** (5) 1569–1578, 2023
https://doi.org/10.1007/s11998-023-00763-w

Two-component UV-curable waterborne CO_2-based polyurethane dispersion with outstanding flexibility

Zhu Ding, Jiahui Chen, Zonglin He, Chaozhi Wang, Hualin Li, Zhenhong Huang, Baohua Liu, Lina Song

Received: 2 October 2022 / Revised: 8 January 2023 / Accepted: 10 January 2023

Abstract A series of two-component UV-curable waterborne CO_2-based polyurethane dispersions (UV-PUDs) with excellent flexibility and mechanical strength were synthesized from poly(propylene carbonate) diol (PPCD), isophorone diisocyanate (IPDI), 2,2-bis(hydroxymethyl) propionic acid (DMPA), 2-hydroxyethyl acrylate (HEA), pentaerythritol triacrylate (PETA) and 1,4-butanediol (BDO). One component was UV-curable waterborne polyurethane terminated by HEA and PETA (molar ratio 1:1), and the other component was linear waterborne polyurethane. The content of the UV-curable component in UV-PUD was 15%, 30%, 45%, 60%, and 100% (weight content). The obtained cured films exhibited superior flexibility without loss of tensile strength, accompanied by excellent acid and alkali resistance. In particular, the dried UV-PUD films without curing showed good mechanical properties.

Keywords UV-curable waterborne polyurethane, Two-component, Poly(propylene carbonate) diol, Flexibility, Acid and alkali resistance

Introduction

UV-curable waterborne polyurethane dispersion (UV-PUD) has the characteristics of fast curing speed, low volatile organic compounds (VOCs), low viscosity, non-toxic, non-flammable and low cost. UV-PUD is widely used in wood and automotive paint, textiles, leather, ink and other fields.[1–5] In the past decades, UV-PUD has been extensively researched.[6–8] However, the existing literature showed that the flexibility and mechanical strength of the cured film were difficult to coexist. The common synthesis method of UV-PUD was to terminate the NCO-end prepolymer with hydroxyethyl acrylate (HEA), hydroxyethyl methacrylate (HEMA), pentaerythritol diacrylate (PEDA), pentaerythritol triacrylate (PETA) and the mixture of acrylic hydroxyl esters.[9–13] The low density of double bonds could bring about excellent toughness, but inferior mechanical strength and chemical resistance of the cured film. Although the mechanical strength could be improved by increasing the content of the double bond, the toughness and adhesion of the cured film extremely decreased. The UV-PUD film synthesized by the common method tended to stick to each other after the evaporation of water. Moreover, the surface properties and mechanical strength of the film was particularly poor in the areas where the ultraviolet light was not available. Therefore, the UV-PUD prepared by the common method is not suitable for the coating of the special-shape parts and applications demanding toughness. In order to solve this problem, Wu et al.[14] proposed that the partial polyurethane prepolymer was terminated by acrylic hydroxyl ester, followed by the reaction of the un-terminated polyurethane prepolymer with the diamine for the chain extension after the neutralization and emulsification process. Some researchers prepared UV-PUD with double bond on the side chain through the reaction between the carboxyl unit of DMPA and the epoxy group of glycidyl methacrylate (GMA). However, the unreactive GMA could react with diamine which was used as the chain extender, which ultimately, could affect the subsequent chain extender reaction and the storage stability. Some researchers synthesized diols with double bonds and then, used the diols as the raw materials to synthesize the UV-PUDs. These ap-

Z. Ding, J. Chen, Z. He, C. Wang,
H. Li, Z. Huang, B. Liu, L. Song (✉)
School of Materials and Energy, Guangdong University of Technology, Guangzhou 510006, Guangdong, People's Republic of China
e-mail: songlina@gdut.edu.cn

proaches were not feasible in industry due to the high cost in the synthesis of the raw material.

In this paper, the acrylic hydroxyl ester and NCO unit terminated polyurethane prepolymers were separately synthesized using poly(propylene carbonate) diol (PPCD) as the raw material. PPCD is derived from carbon dioxide and propylene-epoxide; therefore, the preparation of UV-PUD used PPCD as the raw material is a way of carbon fixation. Two kinds of polyurethane prepolymers were mixed and then followed by the neutralization, emulsification and chain extension process. Finally, the UV-PUDs consisting of two components were prepared. One component terminated by HEA and PETA (molar ratio 1:1) provided the curable double bond under the ultraviolet light. The other component formed waterborne polyurethane with the long chain, which provided the toughness of the cured film. The obtained cured films exhibited excellent flexibility, adhesion of waterborne polyurethane dispersion, outstanding mechanical strength and chemical resistance of UV curable waterborne polyurethane dispersion. Meanwhile, the dry film without carrying out the crosslinking reaction had good mechanical strength and surface properties. Therefore, two-component UV-curable waterborne CO_2-based polyurethane dispersion has the potential applications in the special-shape parts and toughness demanded coatings.

Experimental

Materials

Poly(propylene carbonate) diol (PPCD) (Mn = 1000 g/mol) and poly(propylene carbonate) diol (PPCD222) (Mn = 2000 g/mol) were provided by Guangdong Dazhi Environmental Protection Technology Co., Ltd. (China). Isophorone diisocyanate (IPDI, AR), stanmous octoate (T-9, AR) and 4-ethoxyphenol (MEHQ, AR) were purchased from Aladdin Chemistry Co., Ltd. 2,2-Bis(hydroxymethyl) propionic acid (DMPA, AR), 2-hydroxyethyl acrylate (HEA), pentaerythritol triacrylate (PETA) and 1,4-butanediol (BDO, AR) were purchased from Shanghai Maclin Biochemical Technology Co., Ltd. (China). N, N-Dimethylformamide (DMF, AR) and ethylenediamine (EDA, AR) were received from Tianjin Zhiyuan Chemical Reagent Co., Ltd. (China). Acetone (AT, AR) was provided by Guangzhou Chemical Reagent Factory (China).

PPCD, PPCD222 and BDO were dehydrated under vacuum at 110°C for 3 h before use. DMPA was dehydrated at 120°C for 4 h prior to use. DMF, HEA, PETA, BDO, and AT were dehydrated by 4 Å molecular sieves prior to use.

Synthesis of UV-PUD

PPCD (37.00 g, 37.0 mmol), DMPA (4.08 g, 30.4 mmol), DMF (12.00 g, 164.2 mmol) and IPDI (30.00 g, 134.9 mmol) were charged into a three-neck flask equipped with a digital stirrer for mixing for approximately 10 min at 30–40°C. Ten drops of T-9 were added into the mixture, and then the mixture was heated up to 90°C to react for 4 h. After that, the temperature of the mixture was reduced to 50°C, and MEHQ (0.0358 g, 0.3 mmol), HEA (8.22 g, 70.8 mmol) and PETA (21.14 g, 70.8 mmol) were added. The temperature of mixture was then raised up to 80°C to react for 4 h. After the reaction, the mixture was cooled to 50°C, and then AT (20.00 g, 344.4 mmol) was added to adjust the viscosity. The obtained prepolymer terminated by HEA and PETA was marked as prepolymer A and sealed for use. The synthetic route is illustrated in Fig. 1.

PPCD222 (69.19 g, 34.6 mmol), DMPA (4.42 g, 33.0 mmol), DMF (15.00 g, 205.2 mmol) and IPDI (30.00 g, 135.0 mmol) were charged into a three-neck flask equipped with a digital stirrer to mix for approximate 10 min at 30–40℃. Eleven drops of T-9 were added into the mixture, and then the mixture was heated up to 90°C to react for 4 h. After the reaction, the temperature of the mixture was reduced to 50°C. BDO (2.60 g, 28.9 mmol) was added, and then the mixture was heated up to 70°C for reacting for 2 h. AT (20.00 g, 344.3 mmol) was added to reduce the viscosity of the prepolymer. The obtained prepolymer termi-

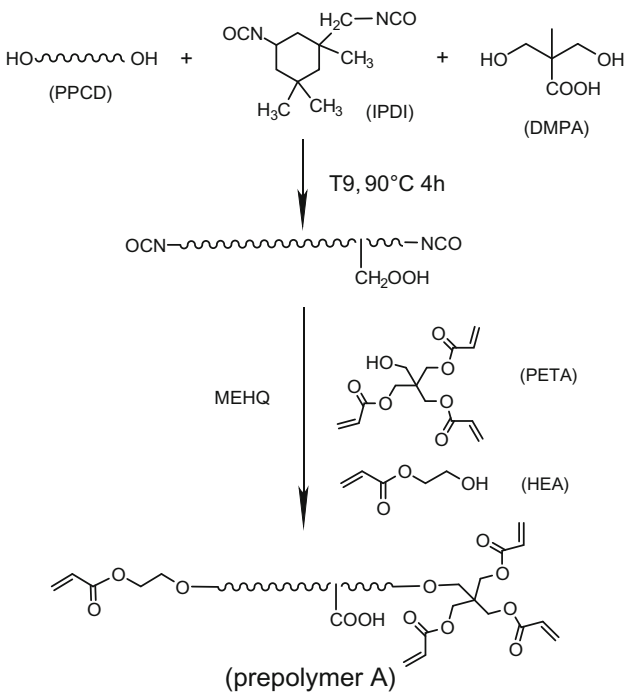

Fig. 1: Synthesis scheme of prepolymer A

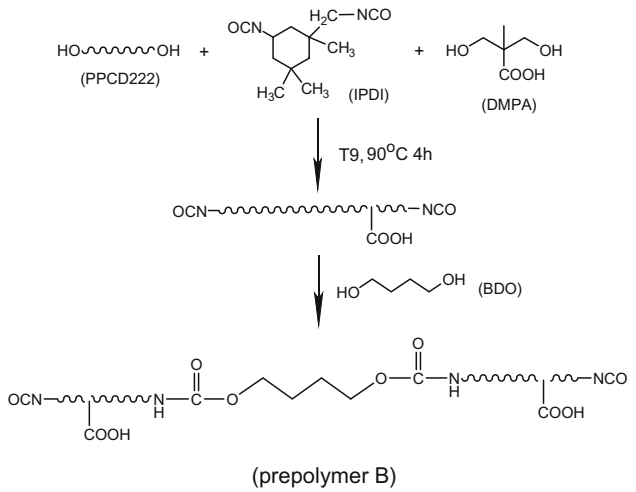

Fig. 2: Synthesis scheme of prepolymer B

nated by NCO unit was marked as prepolymer B, and the synthetic route is shown in Fig. 2.

Prepolymer A and prepolymer B were mixed in a three-neck flask equipped with a digital stirrer at various ratio (the weight content of prepolymer A was 100%, 60%, 45%, 30% and 15%, respectively) to form a homogeneous mixture, followed by the neutralization process using TEA as the neutralizer. After the neutralization, the mixture was poured into cold deionized water (approximately 5°C) to carry out the emulsification process at 2000 rpm for 15 min. After that, stoichiometric EDA diluted by deionized water was added to perform the chain extension process for 30 min. Acetone was then removed at 55°C for 3 h under normal pressure. The UV-PUD emulsion was obtained after the addition of photoinitiator Irgacure 2959 (4.5 wt%). The synthetic route is illustrated in Fig. 3, and the reaction proportions are listed in Table 1.

Preparation of UV-PUD Film

Some certain amount of UV-PUD sample was separately coated onto the polypropylene and tinplate with a 150 μm coater. The coatings were stored at room temperature until the surface was dried, and then dried at 80°C for 12 h. The uncured films were obtained. The uncured films carried out the curing process under 365 nm UV irradiation at 600 mW/cm^2 for 30 s to form the cured films. The emulsion coated on the tinplate performed the curing procedure more than three times to ensure the thickness for the flexibility testing. Another certain amount of UV-PUD sample was evenly coated onto a bidirectional stretch polypropylene film (BOPP) with an 80 μm coater. The uncured films were prepared in the same method mentioned above. Then the curing process of the coating on the BOPP film was monitored by a real-time infrared spectroscopy, and the conversion rate of double bond

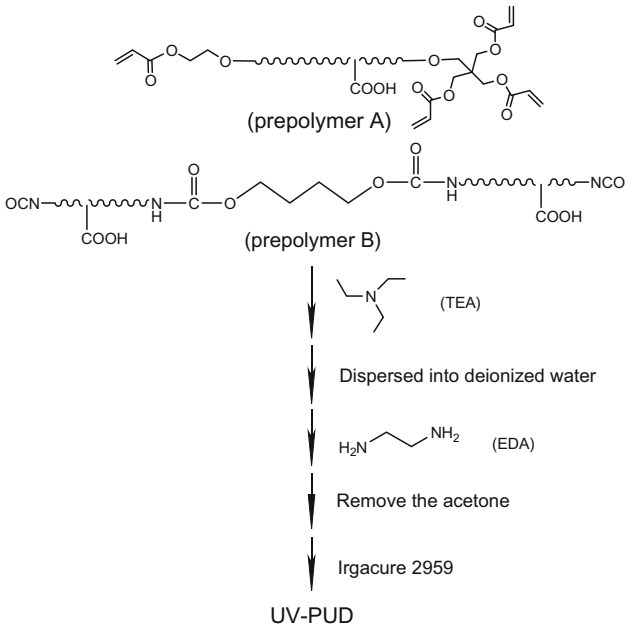

Fig. 3: Synthetic route of UV-PUD

was calculated. The UV intensity was 80 mW/cm^2, and the illumination time was 180 s.

Characterization

A fourier transform infrared spectrometer (FTIR) (Sainz Instruments Co., Ltd., N6700) was used to characterize the structure of the polyurethane prepolymers terminated by hydroxyl acrylate esters at a resolution of 2 cm^{-1} over a wavenumber range of 4000 cm^{-1}∼400 cm^{-1}. The attenuated total reflection (ATR) technique was used to analyze the UV-PUDs films at a resolution of 2 cm^{-1} over a wavenumber range of 4000 cm^{-1}∼650 cm^{-1}. The unsaturation conversions of UV-PUDs during the curing process were monitored by a real-time infrared spectroscopy. The light density at the sample was 80 mW/cm^2, and the duration time was prolonged to 180 s. The conversion percentage of double bond was calculated according to the following equation:

$$\text{Conversion}(\%) = \frac{A_{810-0} - A_{810-C}}{A_{810-0}} \times 100\%$$

where $A_{810\text{-}0}$ and $A_{810\text{-}C}$ were separately the intensity of peak of 810 cm^{-1} before and after UV-curing.

Particle sizes and distributions of UV-PUDs were analyzed by Zeta potential analyzer (Backman Coulter) at room temperature. The solid content of UV-PUD was controlled to be 3-5 wt% with deionized water. The experiment was carried out 3 times and the average was taken as the final value.

Table 1: Reactant proportion of UV-PUDs

	UV-PUD 1	UV-PUD 2	UV-PUD 3	UV-PUD 4	UV-PUD 5
Prepolymer A /g	70	42	31.5	21	10.5
Prepolymer B /g	0	28	38.5	49	59.5
TEA /g	1.67	1.69	1.69	1.69	1.70
H_2O /g	104	103	102	102	97
EDA /g	–	0.20	0.27	0.30	0.42
2959 /g	2.54	1.52	1.14	0.76	0.38
Weight content of prepolymer A	100%	60%	45%	30%	15%

Adhesion of the cured film on the tin plate was tested according to the cross-cut adhesion test method (ASTM D3359).

Water and solvent absorption tests were performed according to the following procedure. The UV-PUD cured films were cut into squares of 20 mm × 20 mm and weighted (m_0). The sample films were immersed in deionized water and solvent for 24 h at room temperature. After the immersion, the water and solvent attached to the films were wiped with filter papers. The film was weighted and recorded as m_1. The water and solvent absorption rate were calculated by the following formula:

$$\text{Absorption rate}(\%) = \frac{m_1 - m_0}{m_0} \times 100\%$$

Gel content of the UV-PUD cured film was tested at room temperature. The films were cut into squares of 20 mm × 20 mm and soaked in anhydrous ethanol. The weight of the film was m_0. After 24 h immersion, the film was dried at 80°C to a constant weight (m_1). The gel content was calculated according to:

$$\text{Gel content}(\%) = \frac{m_1}{m_0} \times 100\%$$

Tensile properties were tested by an electronic universal tensile testing machine (CMT4204, MTS Company) at room temperature according to ASTM D412-1998–2002. The film was cut into the dumbbell type sample with a length and width of 25 and 4 mm, respectively. The testing rate was 200 mm/min.

The acid, alkali and salt resistances of the cured films were measured at room temperature. The dumbbell type samples with a length and width of 25 mm and 4 mm were immersed in the solutions of 10% sulfuric acid, 10% sodium hydroxide and 10% sodium chloride, respectively. After 24 h immersion, the samples were taken out and dried at 80°C to a constant weight. And then, the tensile strength was tested.

Wear resistance of the film was measured according to ASTM D4060-2010.

Flexibility of the film was tested according to ISO 1519–2011.

Thermodynamic stability of the UV-PUD film was detected by a thermogravimetric analyzer (SDT-2960, TA, USA) under nitrogen atmosphere (flow rate: 20 mL/min). The heating rate was 10°C/min, and the heating range was 30∼700°C.

Glass transition temperature of UV-PUD cured films was determined using differential scanning calorimetry (DSC3, METTLER TOLEDO, Switzerland) under nitrogen atmosphere (flow rate: 20 mL/min). The heating rate was 10°C/min at the temperature ranges of −30∼60°C.

Results and discussion

FTIR analysis

FTIR was used to monitor the variation of the functional groups with the reaction time. Figure 4 shows the FTIR spectra of the prepolymer terminated by HEA and PETA after reacting for 3 and 4 h. The characteristic peaks at 3338 and 1533 cm^{-1} could be assigned to the stretching vibration and bending vibration of the N–H group and C-N group, respectively. The peak at 1724 cm^{-1} was attributed to the stretching vibration of the C=O group. These characteristic absorption peaks indicated the formation of urethane groups through the reactions of isocyanate groups and hydroxyl groups.[15] It can be seen that the NCO characteristic peak at 2270 cm^{-1} was visible when the capping reaction lasted for 3 h, which indicated the presence of unreacted isocyanate group (–NCO) in the prepolymer. When the reaction lasted for 4 h, the NCO characteristic peak nearly disappeared, which indicating the complete reaction of the NCO group. Particularly, to prevent the reaction of the double bond, the inhibitor (MEHQ 0.1 wt%) was added into the reaction mixture. An excess of 5% HEA and PETA mixture was used to ensure the complete reaction of the NCO unit.[16]

Figure 5 showed the FTIR spectra of UV-PUD cured and uncured films. Since the UV-PUD1 uncured

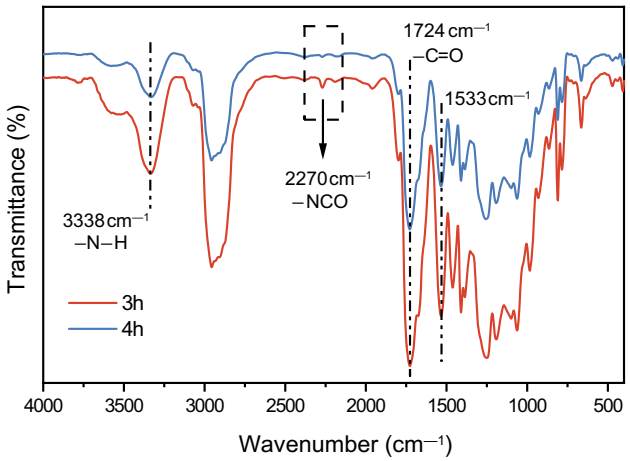

Fig. 4: FTIR spectra of prepolymer terminated by HEA and PETA

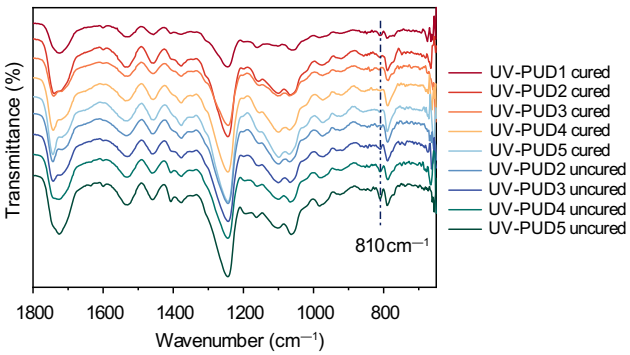

Fig. 5: FTIR spectra of UV-PUD cured and uncured films

film was sticky, the FTIR spectrum of UV-PUD1 uncured film is not presented in Fig. 5. Compared to that of uncured films, the peaks of cured films at 810 cm^{-1} were not obvious, indicating the reaction of double bond upon the exposure of UV light.

Effect of photoinitiator dosage on unsaturation conversion

The properties of the UV-PUD cured films strongly depend on the final unsaturation conversion of double bond after the UV irradiation. The photoinitiator dosage and duration time affect the unsaturation conversion. Irgacure 2959 was used as the photoinitiator of UV-PUD1, and the effect of the weight content on the unsaturation conversion was discussed. The weight content of Irgacure 2959 was 3, 3.5, 4, 4.5 and 5 wt%, respectively. Irgacure 2959 was dissolved in anhydrous ethanol to form a homogenous mixture prior to being added into the UV-PUD1 emulsion. To prevent the oxygen inhibition, the UV-PUD film coated on the BOPP film was covered with another BOPP film. The slope of the conversion curve at the initial curing stage represents the UV-curing rate, and

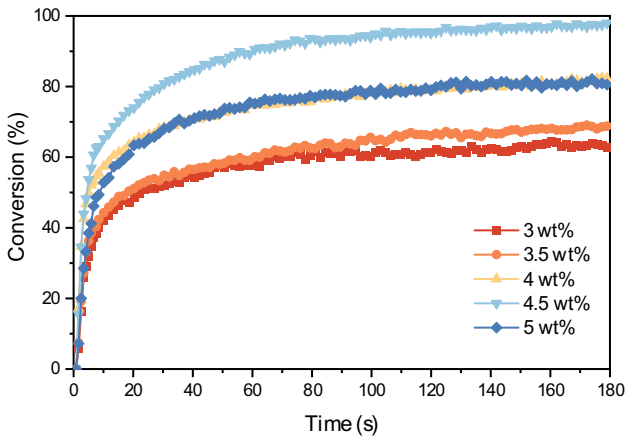

Fig. 6: Effect of photoinitiator dosage on unsaturation conversion of UV-PUD1

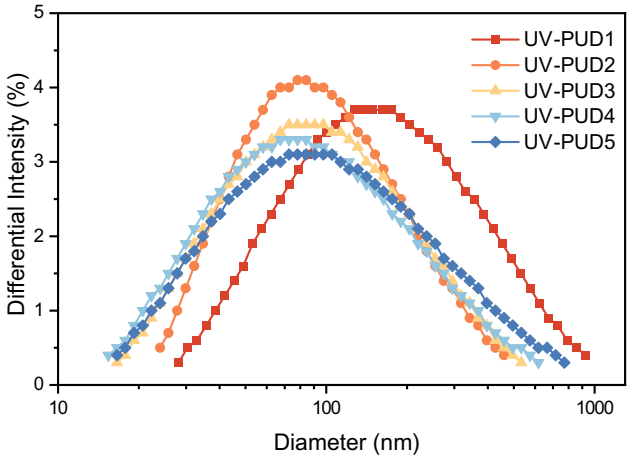

Fig. 7: Particle diameter distributions of UV-PUDs

the plateau value at the final of curing stage indicates the ultimate conversion.[17,18] As shown in Fig. 6, with the increase in Irgacure 2959 dosage, the unsaturation conversion rate gradually increased from 64% to 98%, and then decreased to 81%. When the content of the photoinitiator was 4.5 wt%, the unsaturation conversion was the highest. A small amount of photoinitiator was not sufficient to initiate the reaction of double bond. Excessive photoinitiator, however, could lead to the coupling reaction of free radicals. Therefore, the optimum content of Irgacure 2959 was 4.5 wt%.

Performances of UV-PUDs

Figure 7 shows the particle diameter distributions of UV-PUD emulsions with different prepolymer B contents. The diameters, polydispersity indexes and storage stability of UV-PUDs are listed in Table 2. The emulsion was considered stable (storage duration> 6 months) when no precipitation appeared after the

centrifugal test at 3000 r/min for 15 min.[19] From Table 2, the average particle diameter of UV-PUDs gradually decreased from 130.0 to 69.6 nm with increasing the content of prepolymer B. All the UV-PUD emulsion showed excellent storage stability.

Unsaturation conversions of UV-PUDs

The unsaturation conversion of the UV-PUD samples were measured and calculated, as shown in Fig. 8. The variation of C=C peak at 810 cm^{-1} with the irradiation time was monitored by a real-time infrared spectroscopy. Under the UV irradiation, the rapid increase in the unsaturation conversion in the first 10 s could be attributed to the rapid crosslink reaction. With the prolongation of the irradiation time, the crosslink network restricted the movement of the molecular chain segments, therefore, resulting in the reduction of the unsaturation conversion. The unsaturation conversion remain unchanged at the later curing stage. When the content of prepolymer B increased, the density of the double bond in the mixture decreased, resulting in the decline of the unsaturation conversion.

Table 2: Performances of UV-PUDs

Sample	Diameter/nm	Polydispersity Index	Storage life
UV-PUD 1	130.0	0.293	>6 months
UV-PUD 2	78.5	0.276	>6 months
UV-PUD 3	73.9	0.289	>6 months
UV-PUD 4	72.8	0.316	>6 months
UV-PUD 5	69.6	0.321	>6 months

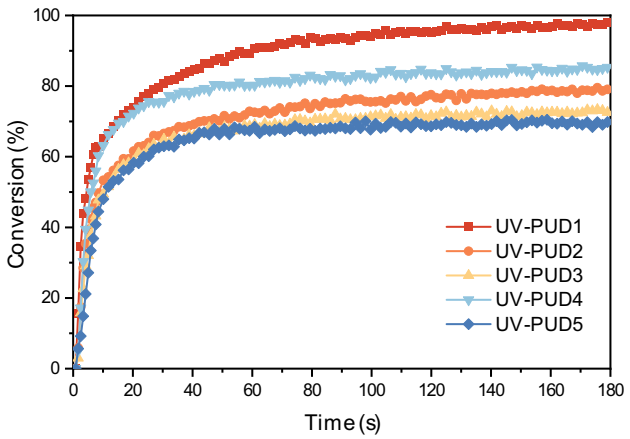

Fig. 8: Dependence of unsaturation conversions of UV-PUDs on irradiation time

Performances of UV-PUD cured films

The adhesion, flexibility, abrasion resistance, water absorption and gel content of UV-PUD films with different prepolymer A contents are shown in Table 3. As can be seen, the UV-PUD cured films exhibited excellent adhesion on the substrates. The flexibility is the ability of coating to adapt to the deformation of substrate, which is related to the comprehensive properties of coating such as toughness, strength and adhesion. The incorporation of prepolyner B improved the flexibility of the cured film. For the UV-PUD1 film on the substrate, the minimum diameter of roll rod was 10 mm, indicating the inferior toughness. For the two-component UV-PUD films (UV-PUD2 to UV-PUD5) on the substrates, the diameters of roll rods were 1 mm (the minimum diameter of the test instrument), illustrating the superior flexibility. Prepolymer A was a component with the double bond at the end of the molecular chain, while prepolymer B was a component with high molecular weight. With the content of prepolymer B increasing, the density of the double bond in the mixture decreased, which resulted in the reduction of the crosslink density in the cured films. Therefore, the gel content and wear resistance decreased, companied by the increase in the water absorption.[20]

Figure 9 shows the absorption rates of the UV-PUD cured films to various solvents, and the data are listed in Table 4. The amount of DMF absorption by the cured film was most sensitive to the crosslinking density among all the solvents. With the crosslinking density decreasing, the amount of solvents absorption by the cured films increased. Among all the solvents, which are listed in Table 4, the UV-PUD cured films had the minimum absorption rate to tetrahydrofuran, while the maximum absorption rate to DMF.

Table 3: Properties of UV-PUD cured films

Sample	Adhesion level	Flexibility/mm	Abrasion resistance/g	Water absorption/%	Gel content/%
UV-PUD1	0	10	0.0105	3.88	91.00
UV-PUD2	0	1	0.0181	7.38	89.08
UV-PUD3	0	1	0.0233	7.53	86.54
UV-PUD4	0	1	0.0258	6.74	87.47
UV-PUD5	0	1	0.0268	12.12	83.23

Table 5 records the mechanical properties and chemicals resistance of UV-PUD films. To further illustrate the advantages of the two-component UV-PUDs, the mechanical properties of UV-PUD films without UV irradiation were also tested. The corresponding stress–strain curves are shown in Fig. 10a and b. UV-PUD1 cured film was too brittle to cut into the testing samples; therefore, the mechanical properties and chemicals resistance were unable to be characterized. The UV-PUDs with different content of prepolymer B had the similar tensile strength. However, the elongation at break gradually increased with the content of prepolymer B increasing. This suggested that component B with long chains provided the flexibility in the two-component UV-PUD cured films.

Conventional UV waterborne polyurethane film without UV irradiation after the evaporation of water exhibited sticky surface and inferior mechanical properties. Consequently, the application of UV-PUD in the special-shape parts was limited. In this research, the obtained UV-PUD cured films without UV irradiation showed certain tensile strength and elongation at break. The tensile strength of UV-PUD2 uncured film containing only prepolymer A was 2.2 MPa. The tensile strength and elongation at break of the UV-PUD5 uncured films were 20.4 MPa and 892%, separately. Due to the high molecular weight, component B provided sufficient mechanical strength and toughness for the uncured films.

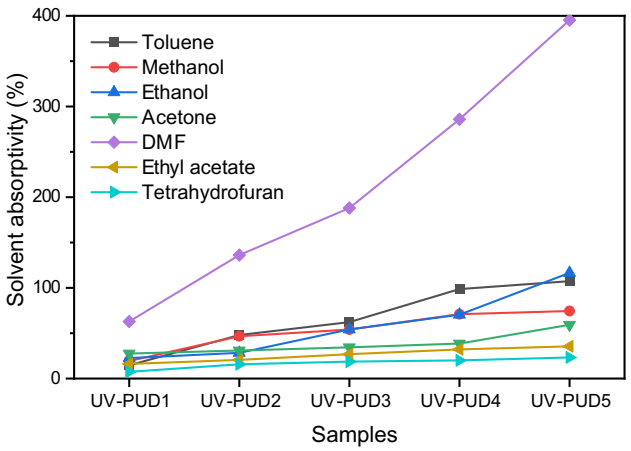

Fig. 9: Solvent absorptivity of UV-PUD cured films

As shown in Table 5, the UV-PUD cured films had excellent acid, alkali and salt resistance. With the content of prepolymer B increased, the acid and alkali resistance of the two-component UV-PUD cured film gradually deteriorated. In our past experiments, the waterborne polyurethane had good acid resistance (70%∼80% stress retention rate) and poor alkali resistance (10%∼20% stress retention rate). Compared to the waterborne polyurethane, the two-component UV-PUD cured films showed excellent acid, alkali and salt resistance.

Thermal properties

Thermal stability of the UV-PUD cured films were determined by TGA. TGA curves of the UV-PUD cured films are shown in Fig. 11. Table 6 lists the characteristic thermal decomposition temperatures of UV-PUD films 5% mass loss ($T_{5\ wt\%}$), 10% mass loss ($T_{10\ wt\%}$), 50% mass loss ($T_{50\ wt\%}$) and the maximum decomposition temperature of two stage (T_{max1} and T_{max2}). Generally, there are two distinct stages in the thermal degradation of polyurethane.[21,22] The first stage in the range of 240∼380°C was attributed to the decomposition of urethane and ether units in the molecular chains. The second stage in the range of 380∼470°C could be due to the decomposition crosslinking bonds and other chemical bonds. Due to the special structure of the carbonate and ether groups in the poly(propylene carbonate) diol molecule, the density of intra-molecular hydrogen bond enhanced with the content of component B increasing. Consequently, the maximum mass loss rate peak at the first stage was improved. On the contrary, the maximum mass loss rate peak at the second stage decreased with the increase in component B, which could be ascribed to the decrease in the crosslink density.

Glass transition temperature of the UV-PUD cured films and PUD film were determined by DSC, and the curves are shown in Fig. 12. Due to the strong polarity of the carbonate group in the structure of PPCD, the phase separation of the soft segments and the hard segments of PUD was inferior, which lead to the single glass transition (−7.6°C) of soft segment in the DSC curve without visible glass transition of the hard segment. However, the content of linear macromolecules in UV-PUD1 was low, so the glass transition

Table 4: Absorption rates of UV-PUD cured films to various solvents

Sample	Toluene/%	Methanol/%	Ethanol/%	Acetone/%	DMF/%	Ethyl acetate/%	Tetrahydrofuran/%
UV-PUD1	14.63	19.32	22.58	27.56	62.86	16.11	7.34
UV-PUD2	47.93	46.69	28.35	30.85	136.11	20.60	15.73
UV-PUD3	62.21	54.04	54.11	34.37	188.07	26.89	18.69
UV-PUD4	98.63	71.01	70.48	38.58	285.93	32.14	19.98
UV-PUD5	107.44	74.48	116.55	59.27	395.32	35.47	23.29

of the hard segment region at 36.6°C appeared in the DSC curve. The glass transitions of UV-PUD2, 3, 4 and 5 were not obvious, which could be attributed to the excellent compatibility between component (A) and component (B).

Conclusions

Two-component UV-PUDs were synthesized using poly(propylene carbonate) diol as raw material. One component (A) was UV-curable waterborne polyurethane terminated by HEA and PETA (molar ratio 1:1), and the other component (B) was linear waterborne polyurethane. The obtained UV-PUD cured films exhibited excellent flexibility, superior adhesion of waterborne polyurethane dispersion, outstanding mechanical strength and chemical resistance of UV curable waterborne polyurethane dispersion. Meanwhile, the dry film without carrying out the crosslinking reaction under the ultraviolet light showed good mechanical strength and surface properties. Therefore, the two-component UV-curable waterborne CO_2-based polyurethane dispersion has the potential appli-

Table 5: Mechanical properties and chemicals resistance of UV-PUDs films

Sample	Cured		Uncured		Acid resistance			
	Strain/%	Stress/MPa	Strain/%	Stress/MPa	Strain/%	Stress/MPa	Strain retention rate[a]	Stress retention rate[b]
UV-PUD2	48	30.1	1181	2.2	10	42.2	21%	140%
UV-PUD3	147	29.7	981	7.2	115	33.0	78%	111%
UV-PUD4	215	32.8	870	11.0	252	35.7	117%	108%
UV-PUD5	417	29.9	892	20.4	423	32.7	101%	109%
Sample	Alkali resistant				Salt resistance			
	Strain/%	Stress/MPa	Strain retention rate	Stress retention rate	Strain/%	Stress/MPa	Strain retention rate	Stress retention rate
UV-PUD2	8	33.3	17%	111%	9	42.3	20%	141%
UV-PUD3	133	28.7	90%	96%	103	27.9	70%	93%
UV-PUD4	188	32.1	87%	97%	187	33.8	87%	102%
UV-PUD5	364	24.4	87%	82%	397	33.6	95%	112%

[a] Strain retention rate: **Strain retention rate** $(\%) = \textbf{resistance strain} \div \textbf{cured strain} \times \textbf{100}\%$

[b] Stress retention rate: **Stress retention rate** $(\%) = \textbf{resistance stress} \div \textbf{cured stress} \times \textbf{100}\%$

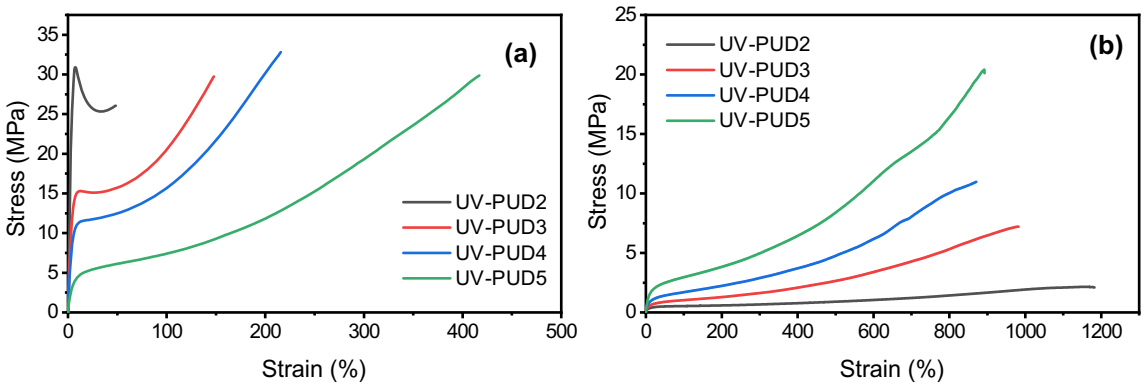

Fig. 10: Stress–strain curves of UV-PUD cured films (a) and uncured films (b)

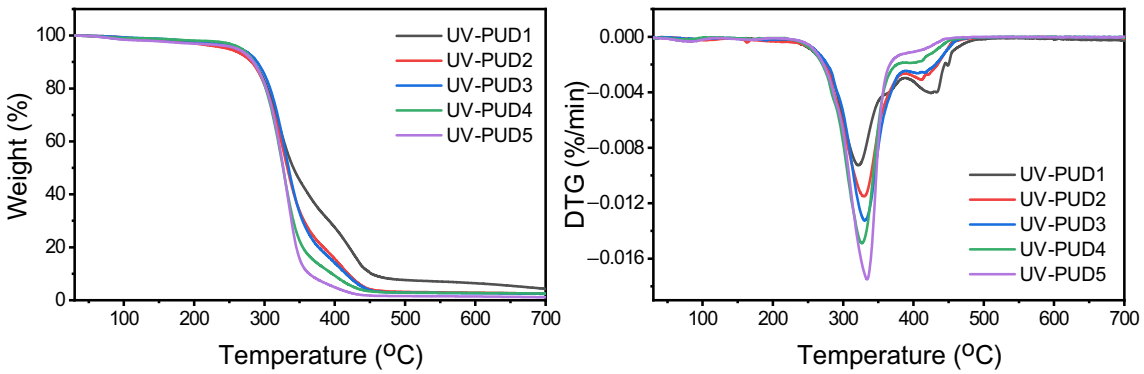

Fig. 11: TGA curves of UV-PUD cured films

Table 6: TGA data of UV-PUD cured films

Sample	$T_{5\ wt\%}$(°C)	$T_{10\ wt\%}$(°C)	$T_{50\ wt\%}$(°C)	T_{max1}(°C)	T_{max2}(°C)
UV-PUD 1	254.6	283.3	341.0	322.3	424.5
UV-PUD 2	248.3	281.6	332.5	328.1	410.7
UV-PUD 3	266.5	289.5	334.3	331.0	404.8
UV-PUD 4	266.8	284.8	326.3	327.1	392.7
UV-PUD 5	261.0	284.1	326.6	334.3	388.2

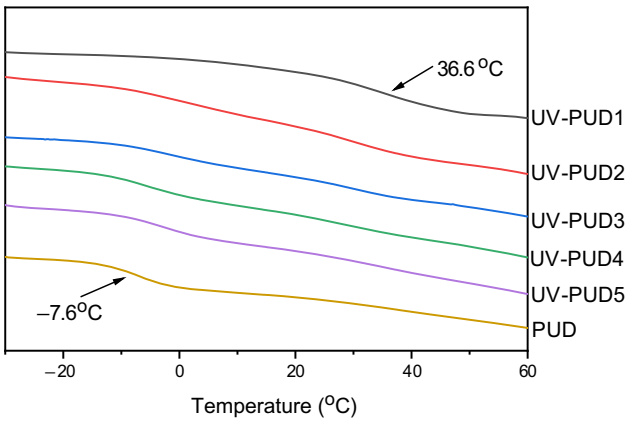

Fig. 12: DSC curves of UV-PUD cured films and PUD film

cations in the special-shape parts and toughness demanded coatings.

Acknowledgments This research did not receive any specific grant from funding agencies in the public, commercial, or not-for-profit sectors.

Conflict of interest The authors declared that we do not have any commercial or associative interest that represents a conflict of interest in connection with the work submitted.

References

1. Li, X, Wang, D, Zhao, LY, et al. "UV LED Curable Epoxy Soybean-Oil-Based Waterborne PUA Resin for Wood Coatings." *Prog. Org. Coat.*, **151** 105942. https://doi.org/10.1016/j.porgcoat.2020.105942 (2021)
2. Ahmed, A, Sarkar, P, Ahmad, I, et al. "Influence of the Nature of Acrylates on the Reactivity, Structure, and Properties of Polyurethane Acrylates." *Ind. Eng. Chem. Res.*, **54** 47–54. https://doi.org/10.1021/ie502953u (2015)
3. Liu, JL, Jiao, XJ, Cheng, F, et al. "Fabrication and Performance of UV Cured Transparent Silicone Modified Polyurethane-Acrylate Coatings with High Hardness, Good Thermal Stability and Adhesion." *Prog. Org. Coat.*, **144** 105673. https://doi.org/10.1016/j.porgcoat.2020.105673 (2020)
4. Li, CH, Xiao, H, Wang, XF, et al. "Development of Green Waterborne UV-Curable Vegetable Oil-Based Urethane Acrylate Pigment Prints Adhesive: Preparation and Application." *J. Clean. Product.*, **180** 272–279. https://doi.org/10.1016/j.jclepro.2018.01.193 (2018)
5. Agnol, LD, Dias, FTG, Ornaghi, HL, et al. "UV-Curable Waterborne Polyurethane Coatings: A State-of-the-Art and Recent Advances Review." *Prog. Org. Coat.*, **154** 106156. https://doi.org/10.1016/j.porgcoat.2021.106156 (2021)
6. Paraskar, PM, Hatkar, VM, Kulkarni, RD, "Facile Synthesis and Characterization of Renewable Dimer Acid-Based Urethane Acrylate Oligomer and Its Utilization in UV-Curable Coatings." *Prog. Org. Coat.*, **149** 105946. https://doi.org/10.1016/j.porgcoat.2020.105946 (2020)
7. Bai, CY, Zhang, XY, Dai, JB, et al. "Water Resistance of the Membranes for UV Curable Waterborne Polyurethane Dispersions." *Prog. Org. Coat.*, **59** (4) 331–336. https://doi.org/10.1016/j.porgcoat.2007.05.003 (2007)

8. Choi, HY, Bae, CY, Kim, BK, "Nanoclay Reinforced UV Curable Waterborne Polyurethane Hybrids." *Prog. Org. Coat.*, **68** (4) 356–362. https://doi.org/10.1016/j.porgcoat.2010.03.015 (2010)
9. Zhang, DL, Liu, J, Li, Z, et al. "Preparation and Properties of UV-Curable Waterborne Silicon-Containing Polyurethane Acrylate Emulsion." *Prog. Org. Coat.*, **160** 106503. https://doi.org/10.1016/j.porgcoat.2021.106503 (2021)
10. Llorente, O, Fernández-Berridi, MJ, González, A, et al. "Study of the Crosslinking Process of Waterborne UV Curable Polyurethane Acrylates." *Prog. Org. Coat.*, **99** 437–442. https://doi.org/10.1016/j.porgcoat.2016.06.020 (2016)
11. Qiu, FX, Xu, HP, Wang, YY, et al. "UV-Curable Waterborne Polyurethane-Acrylate: Preparation, Characterization and Properties." *Prog. Org. Coat.*, **73** (1) 47–53. https://doi.org/10.1016/j.porgcoat.2011.08.019 (2012)
12. Bai, CY, Zhang, XY, Dai, JB, "Synthesis and Characterization of PDMS Modified UV-Curable Waterborne Polyurethane Dispersions for Soft Tact Layers." *Prog. Org. Coat.*, **60** 63–68. https://doi.org/10.1016/j.porgcoat.2007.07.003 (2007)
13. Song, SC, Kim, SJ, Park, KK, et al. "Synthesis and Properties of Waterborne UV-Curable Polyurethane Acrylates using Functional Isocyanate." *Mol. Cryst. Liq. Cryst.*, **659** 40–45. https://doi.org/10.1080/15421406.2018.1450824 (2017)
14. Wu, KH, Xiang, SL, Zhi, WQ, et al. "Preparation and Characterization of UV Curable Waterborne Poly(urethane-acrylate)/Antimony Doped tin Oxide Thermal Insulation Coatings by Sol-Gel Process." *Prog. Org. Coat.*, **113** 39–46. https://doi.org/10.1016/j.porgcoat.2017.08.004 (2017)
15. Hong, CQ, Zhou, X, Ye, YC, et al. "Synthesis and Characterization of UV-Curable Waterborne Polyurethane-Acrylate Modified with Hydroxyl-Terminated Polydimethylsiloxane: UV-Cured Film with Excellent Water Resistance." *Prog. Org. Coat.*, **156** 106251. https://doi.org/10.1016/j.porgcoat.2021.106251 (2021)
16. Wang, J, Zhang, HM, Miao, YY, et al. "UV-Curable Waterborne Polyurethane from CO_2-Polyol with High Hydrolysis Resistance." *Polymer*, **100** 219–226. https://doi.org/10.1016/j.polymer.2016.08.039 (2016)
17. Hwang, HD, Park, CH, Moon, JI, et al. "UV-Curing Behavior and Physical Properties of Waterborne UV-Curable Polycarbonate-Based Polyurethane Dispersion." *Prog. Org. Coat.*, **72** (4) 663–675. https://doi.org/10.1016/j.porgcoat.2011.07.009 (2011)
18. Sangermano, M, Lak, N, Malucelli, G, et al. "UV-Curing and Characterization of Polymer-clay Nanocoatings by Dispersion of Acrylate-Funtionalized Organoclays." *Prog. Org. Coat.*, **61** 89–94. https://doi.org/10.1016/j.porgcoat.2007.09.009 (2008)
19. Yuan, C, Wang, M, Li, H, Wang, Z, "Preparation and Properties of UV-Curable Waterborne Polyurethane-Acrylate Emulsion." *J. Appl. Polym. Sci.*, **134** (34) 45208. https://doi.org/10.1002/app.45208 (2017)
20. Dai, JY, Ma, SQ, Wu, YG, et al. "High Bio-Based Content Waterborne UV-Curable Coatings with Excellent Adhesion and Flexibility." *Prog. Org. Coat.*, **87** 197–203. https://doi.org/10.1016/j.porgcoat.2015.05.030 (2015)
21. Li, KB, Shen, YD, Fei, GQ, "Preparation and Properties of Castor Oil/Pentaerythritol Triacrylate-Based UV Curable Waterborne Polyurethane Acrylate." *Prog. Org. Coat.*, **78** 146–154. https://doi.org/10.1016/j.porgcoat.2014.09.012 (2015)
22. Hwang, HD, Kim, HJ, "UV-Curable Low Surface Energy Fluorinated Polycarbonate-Based Polyurethane Dispersion." *J. Colloid Interf. Sci.*, **362** 274–284. https://doi.org/10.1016/j.jcis.2011.06.044 (2011)